Research papers

Composition and fluxes of submarine groundwater along the Caribbean coast of the Yucatan Peninsula

Kimberly A. Null [a,*], Karen L. Knee [a,b], Elizabeth D. Crook [a], Nicholas R. de Sieyes [c], Mario Rebolledo-Vieyra [d], Laura Hernández-Terrones [d], Adina Paytan [a]

[a] Institute of Marine Sciences, University of California Santa Cruz, 1156 High Street, Santa Cruz, CA 95064, United States
[b] Department of Environmental Science, American University, 4400 Massachusetts Avenue NW, Washington, DC 20016, United States
[c] Department of Land, Air, and Water Resources, University of California Davis, One Shields Avenue, Davis, CA 95616, United States
[d] Centro de Investigación Científica de Yucatán, Unidad de Ciencias del Agua, Calle 8 #39, L1 Mz29 SM64, Cancún, Quintana Roo, Mexico

ARTICLE INFO

ABSTRACT

Submarine groundwater discharge (SGD) to the coastal environment along the eastern Yucatan Peninsula, Quintana Roo, Mexico was investigated using a combination of tracer mass balances and analytical solutions. Two distinct submarine groundwater sources including water from the unconfined surficial aquifer discharging at the beach face and water from a deeper aquifer discharging nearshore through submarine springs (ojos) were identified. The groundwater of nearshore ojos was saline and significantly enriched in short-lived radium isotopes (^{223}Ra, ^{224}Ra) relative to the unconfined aquifer beach face groundwater. We estimated SGD from ojos using ^{223}Ra and used a salinity mass balance to estimate the freshwater discharge at the beach face. Analytical calculations were also used to estimate wave set-up and tidally driven saline seepage into the surf zone and were compared to the salinity-based freshwater discharge estimates. Results suggest that average SGD from ojos along the Yucatan Peninsula Caribbean coast is on the order of 308 m^3 d^{-1} m^{-1} and varies between sampling regions. Higher discharge was observed in the southern regions (568 m^3 d^{-1} m^{-1}) compared to the north (48 m^3 d^{-1} m^{-1}). Discharge at the beach face was in the range of 3.3–8.5 m^3 d^{-1} m^{-1} for freshwater and 2.7 m^3 d^{-1} m^{-1} for saline water based on the salinity mass balance and wave- and tidally-driven discharge, respectively. Although discharge from the ojos was larger in volume than discharge from the unconfined aquifer at the beach face, dissolved inorganic nitrogen (DIN) was significantly higher in beach groundwater; thus, discharge of this unconfined beach aquifer groundwater contributed significantly to total DIN loading to the coast. DIN fluxes were up to 9.9 mol d^{-1} m^{-1} from ojos and 2.1 mol d^{-1} m^{-1} from beach discharge and varied regionally along the 500 km coastline sampled. These results demonstrate the importance of considering the beach zone as a significant nutrient source to coastal waters for future management strategies regarding nutrient loading to reef environments and coastal development. This study also identifies the importance of understanding the connectivity of submarine spring discharge to the nearshore coastal environment and the impact of inland anthropogenic activities may have on coastal health.

© 2014 Elsevier Ltd. All rights reserved.

1. Introduction

Submarine groundwater discharge (SGD), the discharge of subterranean fresh water and recirculated seawater to the coastal zone, occurs throughout the world's coastlines and has been identified as an important source of nutrients to many coastal ecosystems (e.g. Corbett et al., 1999; de Sieyes et al., 2008; Knee et al., 2010; Paytan et al., 2006; Slomp and Van Cappellen, 2004). Many studies have documented the impact of SGD in different environments (Burnett et al., 2003; Moore, 2010; Taniguchi et al., 2006), however SGD in karst environments may be particularly important due to rapid recharge and channelized flow pathways through fractures and cave systems. Specifically two types of flows may be present in karst systems: (1) focused fracture flow (conduits), and (2) diffuse flow through porous medium (Fleury et al., 2007; Moore et al., 1993; Perry et al., 2002). Conduit flow from deeper aquifers may discharge as submarine springs off-shore. Along the Yucatan Peninsula submarine springs (locally known as ojos) are natural features of carbonate dissolution and are linked to extensive underground cavern systems (Beddows et al., 2002, 2007). Diffuse flow from SGD is also evident in the surf zone and includes freshwater from meteoric sources and recirculated seawater from tidal pumping and wave set-up.

Submarine spring discharge in coastal karst systems can be fresh or saline depending on the geology, hydraulic head, rainfall, and extent of subsurface mixing with intruded seawater (Bonacci and Roje-Bonacci, 1997; Fleury et al., 2007). High infiltration rates and rapid flow make aquifers and coastal ecosystems in karst environments vulnerable to anthropogenic pollution including agricultural fertilizers, urban runoff, and untreated sewage from leaking septic systems and/or a lack of wastewater treatment facilities (ArandaCirerol et al., 2011). Volume and constituent loading from submarine springs to nearshore marine environments are difficult to quantify because karst connectivity can be an intrinsic system of open conduits with focused discharge points that vary greatly in space, magnitude, and quantity within one region (Fleury et al., 2007). There is a need to better understand how anthropogenic activity and groundwater delivery in areas with karst geology are linked to land use and pollutant transport that impact local coastal ecosystems.

Groundwater flow and discharge to the Yucatan Peninsula coast has been estimated using regional water balance considerations for the Peninsula as a whole (Hanshaw and Back, 1980), for the north coast (Smith et al., 1999), and for the east coast (Beddows et al., 2002) and the potential impact of associated nutrient loads was recognized (Herrera-Silveira, 1998). Nitrogen (N) is often the limiting nutrient in coastal marine environments although phosphorus (P) discharge to nearshore environments in karst regions is extremely low because of interactions with calcium carbonate (Fourqurean et al., 1993), thus P may also be of interest in these systems. Specifically, nutrient ratios of the discharging water may affect productivity and species abundance and distribution in coastal ecosystems in karst settings. Furthermore, human impact may alter the natural nutrient ratios through agriculture and development both along the coastline and inland at the recharge areas.

Anthropogenic activities that increase nutrient delivery to coastal waters are responsible for shifts in phytoplankton community structure and degradation in the health of coral reefs and seagrass beds throughout the world (Chérubin et al., 2008; Haynes et al., 2007; Paytan et al., 2006). In the Yucatan Peninsula, rapid population growth and development, tourism, and agricultural practices with intensive fertilizers have increased pressures on coastal resources and have raised concerns about groundwater pollution and overall coastal ecosystem health (Metcalfe et al., 2011). The objectives of this study are to quantify SGD contributions from both the beach face and ojos along the eastern coast of the Yucatan Peninsula and to estimate the nutrient fluxes to the nearshore coastal reef environments associated with SGD. Four sites located in different geomorphological regions and with different land-use practices were selected to determine regional and site specific fluxes and relate them to human activities near the coast.

2. Methods

2.1. Study region

Four sites (Cancun, Puerto Morelos, Sian Ka'an, and Xcalak) located in the state of Quintana Roo that borders the Caribbean Sea on the eastern coast of the Yucatan Peninsula were sampled (Fig. 1). The Yucatan Peninsula is a low-relief limestone platform. The south central area has the highest elevation, up to 250 m above sea level. The rainy season in the region is between June and October and precipitation ranges from 900 to 1500 mm yr^{-1} (Chavez-Guillen, 1986; Perry et al., 2002). The area is characterized by minimal surface runoff due to high infiltration rates but a lag of several months may exist before peak discharge of groundwater to the coast occurs (Michael et al., 2005; Perry et al., 1989).

The Yucatan Peninsula can be divided into six regions based on hydrogeochemical and physiographic characteristics (Perry et al., 2002). The hydrogeochemical zonation of the Peninsula is based on differences in tectonic history, rainfall, rock type, and erosion (Perry et al., 1995). Cancun, Puerto Morelos (PM), and Sian Ka'an are located in the Holbox Fracture Zone/Xel Ha Zone, whereas Xcalak is located in the "Evaporite Region" (Perry et al., 2002). Recent studies suggest that Sian Ka'an is located in the Rio Hondo
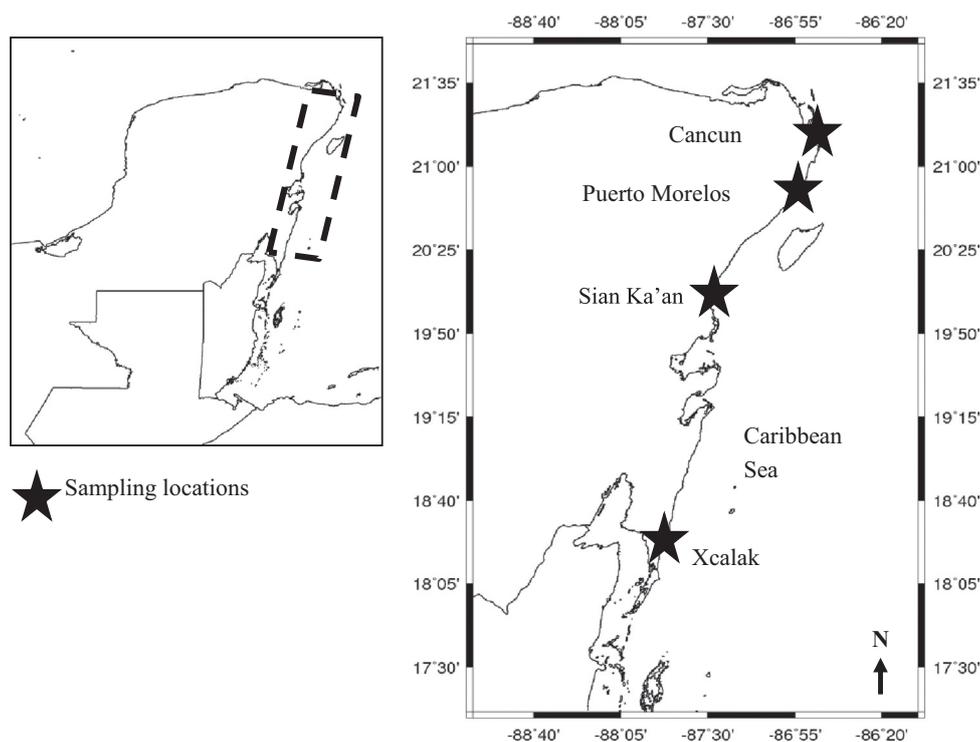

Fig. 1. Map of the four sampling sites (Cancun, Puerto Morelos, Sian Ka'an, and Xcalak) located along the eastern Yucatan Peninsula, Mexico bordering the Caribbean Sea.

fracture zone that intersects the Holbox fracture zone near Tulum, and therefore may represent a unique groundwater system (Gondwe et al., 2010a). Each hydrogeochemical zone is characterized by a different degree of bedrock fracturing which may influence the direction and magnitude of groundwater flow (Isphording, 1975). Indeed it has been noted that groundwater flow is different between the regions; in the Holbox Fracture Zone groundwater flow is predominately to the northeast and in the Evaporite Region flow direction is to the southeast (Perry et al., 2002). The Holbox Fracture Zone consists of sabanas (solution depressions) that are aligned in chains > 100 km long that follow offshore tectonic structures. The Evaporite Region, as the name implies, has evaporite units dispersed within the limestone formation and it is geomorphologically different than the rest of the Yucatan with the presence of swamps and some ephemeral streams.

Development, population growth, and tourism along the Caribbean coast of the Yucatan Peninsula have resulted in increased pressure on water resources. Groundwater is the only freshwater source for this region of Mexico and is found within a freshwater lens ~10–100 m thick depending on location, typically thinning near the coast (Beddows et al., 2002). Below the freshwater lens, seawater intrusion can occur up to 100 km inland (Back and Hanshaw, 1970; Beddows et al., 2007; Steinich and Marín, 1996; Stoessell et al., 1989), potentially exacerbating the impact of groundwater withdrawal and pollution from development and population growth. Cancun is a heavily populated and highly developed area that is a major tourist destination (> 700,000 residents; Instituto Nacional de Estadistica y Geografia, www.inegi.org.mx; > 7 millions of tourist; Secretaría de Turismo de Quintana Roo, http://www.sedetur.qroo.gob.mx). Puerto Morelos is a fishing village located ~35 km south of Cancun, but increased tourism and urban development in the past few decades have intensified the demand on water resources. The town of Puerto Morelos has grown from ~700 permanent residents in 1980 to > 9000 in 2010 (Instituto Nacional de Estadistica y Geografia, http://www.inegi.org.mx), and there are no sewage treatment facilities in many parts of inland Puerto Morelos (Ruiz-Renteria et al., 1998). Tourism development is expanding in Puerto Morelos with > 1.7 million tourists visiting the Riviera Maya every year and migrating farther south from Cancun to visit the unique ecological systems (Meacham, 2007). Sian Ka'an is a biosphere reserve located approximately 120 km south of Cancun that is ecologically important because it is a groundwater fed wetland ecosystem. The town of Tulum is located just north of the reserve but has a small population (~18,000 inhabitants in 2010) and some hotels along the coast (Instituto Nacional de Estadistica y Geografia, http://www.inegi. org.mx). The southernmost site, Xcalak, is a very small village (population of 375 inhabitants) located 240 km south of Tulum. Only 32% of the population in the State of Quintana Roo utilizes municipal wastewater treatment systems, with decreasing availability of treatment systems in southern municipalities (e.g. 14% of population in the Municipality of Solidaridad, south of Cancun and includes the ecotourism park Xcaret; Metcalfe et al., 2011). Common practice is to pump sewage below the freshwater lens into the saline zone for discharge to the coast (Metcalfe et al., 2011).

The sampling locations used in this study represent a gradient of decreasing population and development and increasing coastal park areas from north to south (Cancun to Xcalak). Notably, despite the smaller population and greater abundance of protected lands towards the south, anthropogenic impacts on freshwater resources and coastal environments may still exist in this section of the Peninsula from intense agriculture inland (Pacheco and Cabrera, 1997). Tourism on the east coast of the Yucatan Peninsula has increased four fold in recent years (~1995–2005) and there is evidence of elevated N concentrations in groundwater that exceed drinking water standards (Hernández-Terrones et al., 2011; Mutchler et al., 2007).
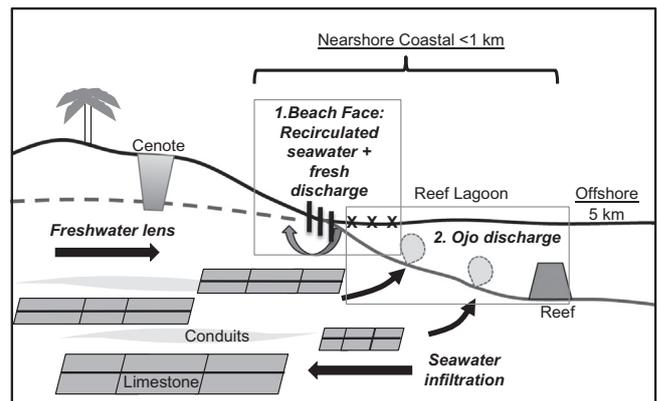

Fig. 2. Schematic diagram representing sampling environment and end-members (beach face groundwater, ojo, reef lagoon in the nearshore zone, and offshore waters). Similar settings were sampled at all four sites along the Yucatan Peninsula to quantify different SGD occurring at the (1) beach face and (2) ojos.

2.2. Sample collection and analyses

Samples were collected at each sampling site (Fig. 1) on four sampling campaigns between January 2009 and November 2009 to characterize the different water end-members present: beach groundwater, nearshore surface water (within the reef lagoon), permanently submerged submarine springs (ojos), and offshore (beyond the reef lagoon) (Fig. 2) along a 12 km coastline for each site. Groundwater at the beach face and surface water samples at each site were collected along 5–10 transects oriented from shore towards open waters throughout the 12 km shoreline (Fig. 2). The 12 km of coastline was defined by the distance between north and south transects at each site. Generally, each nearshore transect consisted of up to six discrete samples, three from temporary screened PVC wells (or pits when a well could not be installed) at the beach face (0.5–1.25 m depth) and three from surface water at increasing distance from shore (up to~1.5 m water depth). The distance from shore each of these transects extended varied at each site depending on beach slope and water depth. Additional nearshore surface water samples were collected within the reef lagoon (≤ 1 km offshore) via boat using a submersible pump. Offshore (beyond the reef crest) surface and bottom water samples were collected at each site at a distance of up to 5 km from shore. Samples from ojos (6–12 ojos per site) found at each of the sampling zones were also collected by divers at underwater discharge points. Samples from all sites were analyzed for radium isotopes (^{223}Ra, ^{224}Ra) and nutrient concentrations ($NO_3^- + NO_2^-$, NH_4^+, PO_4^{3-}, SiO_2). Water characteristics (salinity, conductivity, temperature) were also measured in the field using a calibrated handheld YSI 85 multi-probe (Yellow Springs Instruments, Inc.). Detailed methods and protocols for the analysis of each parameter are described below.

2.2.1. Radium

Groundwater (40–60 L each sample) and surface water samples (100 L each sample) were collected using submersible pumps and passed through MnO_2-coated acrylic fiber at a flow-rate- < 2 L min^{-1} to scavenge the Ra isotopes (Moore, 1976). The fibers were rinsed with Ra-free water and immediately shipped to the University of California Santa Cruz (UCSC) for analysis. Short-lived radium isotope activities (^{223}Ra and ^{224}Ra) were measured using a delayed-coincidence counter (RaDeCC) at UCSC (Moore and Arnold, 1996). The fibers were analyzed a second time, approximately 4 weeks after collection, to measure ^{228}Th and correct for supported ^{224}Ra (Moore, 1976; Moore, 2000). Standards are measured on the RaDeCC systems on a monthly basis as part of

the quality control protocol of the instrument and to calculate efficiencies. The analytical error of the calculated efficiencies of the RaDeCC systems is typically $< 10\%$. The average error associated with the measurement of ^{224}Ra and ^{223}Ra activities for all groundwater and nearshore samples analyzed here is 6% and 15%, respectively, based on calculations following Garcia-Solsona et al. (2008).

2.2.2. Nutrients

Samples for nutrient concentrations ($NO_3^- + NO_2^-$, NH_4^+, PO_4^{3-}, SiO_2) were filtered with 0.45 μm syringe filters and collected in acid cleaned polyethylene bottles. Nutrient samples were frozen until analyzed colorimetrically using a Lachat Quickchem 8000 Flow Injection Autoanalyzer at UCSC. Analytical error was $< 10\%$ for all nutrients based on duplicate samples analyzed every ten samples.

2.3. SGD flux calculations

Brackish SGD fluxes from ojos were calculated based on excess Ra activities in the nearshore coastal zone (< 1 km) using a Ra mass balance model (Moore, 1996). Excess Ra activities were determined and discharge fluxes calculated separately for each of the four sampling locations. The Ra mass balance model accounts only for the discharge from the brackish ojos (e.g. cumulative discharge from all ojos to the coastal zone) and does not include the diffuse freshwater discharge from the unconfined coastal aquifer. To quantify the saline discharge occurring at the beach face we used analytical calculations to establish a first order approximation of SGD from wave set-up (Longuet-Higgins, 1983) and tidal pumping (Li et al., 1999), and salinity end-member mixing models for freshwater discharge. The different SGD end-members (ojo, beach groundwater, nearshore, and offshore) can be distinguished geochemically (discussed in Section 3) and are represented in Fig. 2.

2.3.1. Ojo discharge

The average Ra activities of ojo groundwater, surface water in the nearshore area where the ojos discharge (reef lagoon), and open ocean surface water (beyond the reef up to 5 km offshore) were used to represent the end-members (defined as ojos, nearshore box, and offshore, respectively) for the box model mass balance mixing calculations (Fig. 2). The SGD flux from the ojos was calculated from Eq. (1) modified from Moore (1996):

$$D_{ojo} = \frac{(V_{box}/\tau)(A_{box} - A_{offshore})}{A_{ojo}} \tag{1}$$

Discharge (D) was calculated from the excess ^{223}Ra activity in the box (above that of the offshore water). ^{223}Ra activity from the beach face was not subtracted from the total excess activity, and

the excess activity is considered as being supplied primarily from SGD from the brackish ojos. We calculate that the average saline and freshwater flux contributes $< 1\%$ to the excess Ra activity in the nearshore environment. $A_{offshore, box, ojo}$ refer to the ^{223}Ra activities (dpm m^{-3}) of each respective end-member; V_{box} is the volume of the box, shaped like a prism to account for beach slope (shore length × water depth just shoreward of the reef × distance to reef × 0.5), which represents the reef lagoon and varies in dimension depending on the sampling location (Table 1); and τ is the water residence time (d) within the coastal box. A site-specific estimate of τ was made for each location based on known reef lagoon dimensions and using a constant water transport of 986 m^3 s^{-1}, a transport value published for Puerto Morelos based on a lagoon volume of 8×10^6 m^3 (Coronado et al., 2007). Each of the coastal regions have different volumes due to differences in water depth and distance to the reef crest from shore, and therefore the residence time for each location was calculated by dividing the volume of the coastal lagoon for each region (coastal box) by this published water transport. τ was calculated for each site and ranged between 0.038–0.492 d (1.5 h–11.8 h). It is reasonable to assume that these calculations provide an adequate estimate of residence times among all sites because similar currents (Yucatan Current) and coastal morphology (reef lagoon) regimes exist throughout the region (Núnez-Lara et al., 2005). These estimates, except for 0.038 d at Xcalak, are within the range of residence times determined using published current speeds along the eastern Yucatan Peninsula: 0.46 d at PM using 600 m^3 s^{-1} (0.15 m s^{-1}; Kjerfve, 1994) and 0.21 d at PM using 1303 m^3 s^{-1} (calculated average of 0.32 m s^{-1}; Merino-Ibarra, 1986).

We used Eq. (1) for the site-specific SGD calculations without considering activity loss due to decay (^{223}Ra decay constant: 0.0608 d^{-1}) since decay is negligible within each box based on the residence time estimates. The assumptions of this model are the following: (1) the system (box) is well-mixed and in steady state, (2) the ojos are the primary source of ^{223}Ra to surface waters, (3) there are no additions of ^{223}Ra besides the source (ojos). We use ^{223}Ra activities as opposed to ^{224}Ra activities to calculate ojo discharge because ojo water has low ^{224}Ra activities relative to ^{223}Ra activities and our results suggest an additional ^{224}Ra source in offshore waters. See Section 4 for further details regarding the use of ^{223}Ra to calculate SGD.

2.3.2. Beach face discharge

We used analytical calculations to establish a first order approximation of SGD occurring at the beach face and within the surf zone. Ra could not be used as a tracer of SGD at the beach face, due to the freshness of many of the groundwater samples (e.g. low Ra) and the elevated Ra activities in surface waters from Ra enriched saline ojo waters discharging nearby. For the purpose of this study fresh groundwater was defined as water with salinity < 7. Below this salinity particle desorption of Ra is minimal and therefore samples with < 7 salinity do not demonstrate the maximum Ra enrichment (freshwater beach groundwater samples exhibit ~40% of Ra found in the saline beach groundwater samples); this imposes constraints on using Ra as a tracer for low salinity water discharge (Webster et al., 1995). SGD occurring at the beach face was calculated based on wave set-up (Longuet-Higgins, 1983), tidal pumping (Li et al., 1999), and freshwater discharge at the beach face using the following equation modified from Li et al. (1999):

$$D_{beach} = D_{wave} + D_{tide} + D_{fresh} \tag{2}$$

D_{wave} and D_{tide} represent seawater circulated through the surficial aquifer in the surf zone; where D_{wave} is the discharge occurring due to wave set-up and can be estimated following the equation from (Longuet-Higgins, 1983)

$$D_{wave} = KSL \tag{3}$$

Table 1
Values of sampling site parameters for the mass balance Ra model including volume of nearshore box (V_{box}), τ (residence time), depth, distance to reef from shore, and approximate length of shoreline for each sampling site.

Site	V_{box} (1×10^6 m^3)	τ (d)[a]	Depth (m)	Approx. distance to reef (m)	Length of shoreline (km)
Cancun	31.5	0.492	5.25	1000	12
PM	24.0	0.375	4.0	1000	12
Sian Ka'an	16.2	0.253	4.5	600	12
Xcalak	2.4	0.038	2.0	200	12

[a] Based on a residence time of 0.125 d for a lagoon volume of 8×10^6 m^3 at Puerto Morelos (Coronado et al., 2007).

In Eq. (3), K is hydraulic conductivity, S is slope of the wave-setup and L is the width of the surf zone (20 m). K was estimated as 12.5 m d^{-1} (the median of 5–20 m d^{-1}) based on grain size of medium sand (Domenico and Schwartz, 1990). Estimates of S can be calculated from the breaker height (0.5 m), wave period (7 s averaged over 45 d during study dates; http://www.ndbc.noaa.gov/station), and beach slope (0.075) using equations in Li et al. (1999). D_{tide} was calculated based on the following equation from Li et al. (1999) and Boehm et al. (2004):

$$D_{tide} = \frac{n_e a}{kT} \exp(-\alpha)(\cos \alpha - \sin \alpha)$$
$$+ \frac{\sqrt{2n_e}a^2}{S_b T} \exp(-\sqrt{2\alpha}) \cos(\sqrt{2\alpha}) + \frac{n_e a^2}{S_b T} \quad (4)$$

where

$$k = \sqrt{\frac{n_e \omega}{2KH}} \quad (5)$$

and

$$\alpha = \frac{ka}{S_b} \quad (6)$$

For Eqs. (4)–(6), n_e is effective porosity and was estimated to be 0.225 (median of 0.15–0.30) based on medium sand grain size (Krekeler et al., 2009; McWhorter and Sunada, 1977); a is tidal amplitude (0.3679 m); T is the tidal period (12.42 h) and ω is tidal frequency (1.41×10^{-4} rad s^{-1}) based on M2 harmonic. H is the beach sand aquifer thickness for recirculated seawater considering tidal wave set-up and tidal pumping through the porous beach sand (average of 2 m; directly measured at temporary well installations); and S_b (0.075) is the beach slope calculated based on the width of the surf zone and the depth during sampling. The input values used to calculate D_{wave} and D_{tide} encompass representative average ranges and may vary at each site. The median value of the ranges for the available data was used and assumed to be similar among sites and therefore should be considered as a first order approximation of the saline groundwater end-member occurring at the beach face.

D_{fresh} was estimated using a salinity mass balance model in the surf zone. It was assumed the surf zone was well mixed. The average surf zone salinities (S_{box}) and average offshore salinities ($S_{offshore}$) were used at each site in the following equation:

$$D_{fresh} = \left(\frac{S_{offshore} - S_{box}}{S_{offshore}} \right) \left(\frac{V_{box}}{\tau L} \right) \quad (7)$$

The mass balance approach was applied to the nearshore surf zone and determined per meter of shoreline (L). The surf zone (for the beach face discharge calculations) extended 20 m offshore at all sites ($V_{box} = 15$ m^3) and we used a residence time of 0.125 d (τ) (Coronado et al., 2007). The residence time is the same at each site since we used the same size surf zone box for each site and the average water depth was similar within 20 m of the shoreline. The residence time we use is the best estimate based on previous studies of currents and exchange rates in the area (Coronado et al., 2007; Kjerfve, 1994; Merino-Ibarra, 1986); however there is limited knowledge of the extent of the Yucatan Current and exchange of water with flooding and ebbing tides within 20 m of shore. We assume the Yucatan Current influences the residence time within 20 m of shore in addition to the influence of tides (semi-diurnal mixed; ~12 h tide cycle). We did not investigate the nature of the fresh groundwater discharge, whether as part of the tidal circulation cell, or as a freshwater "tube"; however, based on the analytical approach in this paper, we assume that freshwater discharges following a pathway or "tube" as opposed to mixing with the tidal recirculation cell (Robinson et al., 2007). This assumption seems valid based on the karst environment that has focal freshwater discharge points and surface runoff is negligible because nearly all precipitation either evaporates or infiltrates and recharges the aquifer in this karst environment (Villasuso and Ramos, 2000).

2.4. Data analysis

Variance among end-members (ojos, beach groundwater, nearshore, and offshore) and sampling locations was analyzed using Kruskal–Wallis nonparametric one-way analysis of variance. Statistical significance was determined using a 95% confidence interval ($p < 0.05$). Statistical analyses were conducted using StatCrunch (Integrated Analytics, LLC).

Table 2
^{223}Ra, ^{224}Ra, and ^{228}Th activity means in disintegrations per minute per 100 liters (dpm 100 L^{-1}) and standard deviations (SD) for each end-member at each site. Salinity and average activity ratios (AR), ^{224}Ra/^{223}Ra, for each end-member are also reported.

Site/Date		n	Salinity		^{223}Ra (dpm 100 L^{-1})		^{224}Ra (dpm 100 L^{-1})		^{228}Th (dpm 100 L^{-1})		AR ($^{224/223}$Ra)
			Ave	SD	Ave	SD	Ave	SD	Ave	SD	Ave
Cancun/Nov 09	**Fresh Beach GW**	6	**2.6**	0.6	**0.05**	0.04	**0.17**	0.09	**0.04**	0.01	**3.5**
	Beach GW	24	**29.6**	8.4	**0.53**	0.40	**2.90**	1.90	**0.10**	0.01	**5.7**
	Nearshore	40	**34.6**	1.6	**0.32**	0.29	**2.97**	1.03	**0.17**	0.07	**13.7**
	Ojo	6	**23.4**	9.1	**13.92**	16.4	**8.75**	6.10	**0.50**	0.04	**0.9**
	Offshore	13	**36.1**	0.3	**0.18**	0.20	**2.9**	1.30	**0.37**	0.13	**26.1**
PM/Jan 09	**Fresh Beach GW**	4	**4.2**	2.4	**0.23**	0.2	**0.97**	0.72	**0.02**	0.03	**6.2**
	Beach GW	5	**13.9**	10.6	**0.32**	0.05	**2.44**	0.46	**0.18**	0.08	**7.7**
	Nearshore	23	**35.9**	0.2	**0.29**	0.13	**3.41**	1.35	**0.21**	0.11	**12.1**
	Ojo	12	**27.8**	7.0	**27.20**	20.9	**15.83**	12.9	**3.91**	4.5	**0.7**
	Offshore	9	**37.6**	0.4	**0.25**	0.12	**3.43**	1.1	**0.24**	0.09	**16.8**
Sian Ka'an/Oct 09	**Fresh Beach GW**	2	**1.1**	0.8	**0.9**	1.2	**5.5**	6.7	**0.28**	0.04	**8.1**
	Beach GW	20	**28.1**	7.8	**1.42**	0.92	**6.98**	4.43	**0.25**	0.19	**5.5**
	Nearshore	36	**31.2**	1.3	**2.76**	1.51	**8.38**	3.4	**0.28**	0.14	**3.8**
	Ojo	7	**16.5**	2.5	**15.46**	20.4	**18.90**	8.93	**2.39**	0.39	**3.1**
	Offshore	0	**NA**	NA	**NA**	NA	**NA**	NA	**NA**	NA	**NA**
Xcalak/Jan 09	**Fresh Beach GW**	7	**3.4**	1.8	**4.76**	1.98	**0.12**	0.05	**0.22**	0.06	**0.1**
	Beach GW	4	**17.1**	3.6	**0.64**	0.27	**1.60**	0.83	**0.13**	0.03	**2.5**
	Nearshore	24	**32.0**	5.9	**0.87**	0.96	**6.50**	2.34	**0.25**	0.12	**14.5**
	Ojo	6	**14.6**	2.6	**18.62**	1.67	**37.06**	10.4	**2.35**	1.53	**2**
	Offshore	8	**35.9**	0.2	**0.12**	0.06	**3.85**	1.50	**0.25**	0.08	**40.1**

3. Results

3.1. Radium activities

A summary of [223]Ra and [224]Ra activities for the different sample groups (beach groundwater, nearshore, ojo, and offshore) at each site is shown in Table 2. The end-members used in the mixing model can be distinguished based on Ra activities. When considering all the Ra activities regardless of location, the [223]Ra and [224]Ra activities were significantly higher in samples from ojos compared to beach groundwater and surface water ($p < 0.001$) (Table 2). We found beach groundwater [223]Ra activities in the range of 0.1–2.7 dpm 100 L^{-1} and the highest [223]Ra activity was measured in ojos (66.4 dpm 100 L^{-1}) with a range of 0.2–66.4 dpm 100 L^{-1}. [224]Ra activities showed similar trends with greater activities in ojos (0.6–51.9 dpm 100 L^{-1}) than in the beach groundwater (0.4–14.7 dpm 100 L^{-1}). [223]Ra and [224]Ra activities were lower in fresh beach groundwater samples (salinity < 7) compared to ojos and saline beach groundwater, except at Xcalak where fresh beach groundwater activities were greater than saline beach groundwater activities (Table 2). All sampled ojos except for one ojo at Sian Ka'an, had salinity > 7. Mean [223]Ra and [224]Ra activities in lagoon surface waters differed between sampling sites (0.03–7.48 dpm 100 L^{-1} and 0.6–14.9 dpm 100 L^{-1}, respectively) but did not show a significant decrease in [223]Ra or [224]Ra activities with distance from shore within the reef lagoon (up to 1000 m depending on the site), indicative of the short residence time of water in the lagoon and the presence of enriched Ra ojo discharge throughout the lagoon (Fig. 3). Beyond the reef there was a significant decrease of [223]Ra and [224]Ra activities in offshore waters at some of the sites. At Cancun, offshore [223]Ra activities were significantly different than nearshore activities ($p < 0.0001$), but
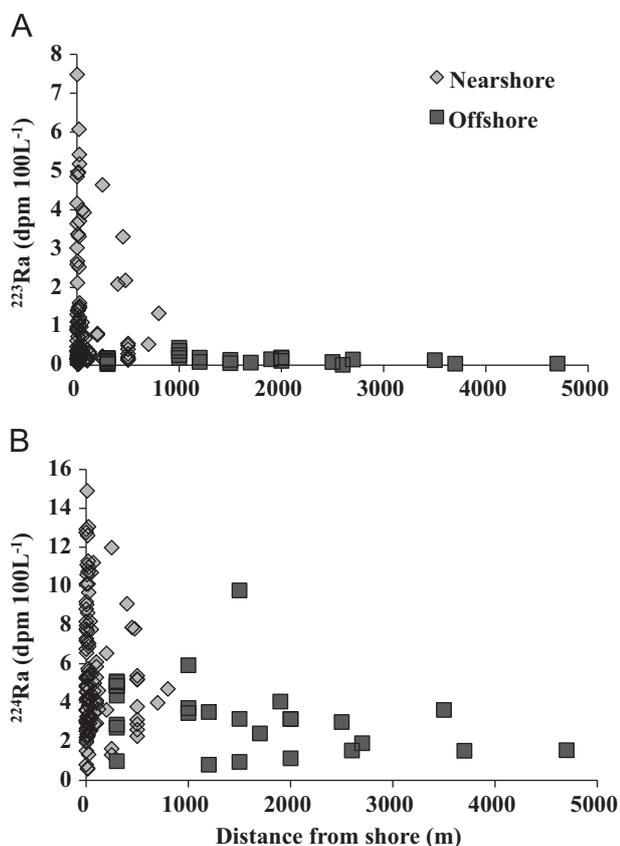

Fig. 3. (a) [223]Ra activities and (b) [224]Ra activities of nearshore and offshore surface water with distance from shore at all sampling locations.
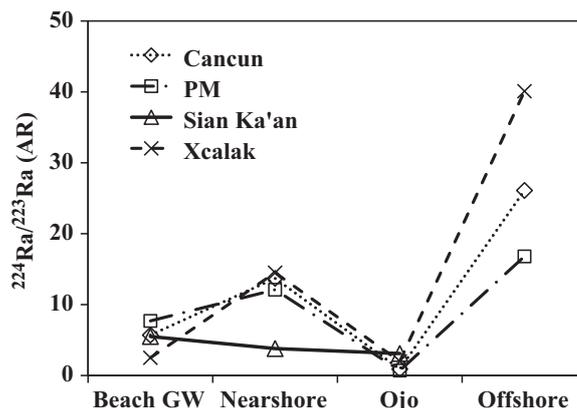

Fig. 4. Average [224]Ra/[223]Ra activity ratio (AR) for each end-member (beach groundwater, nearshore, ojo, and offshore) at each of the sampling locations.

[224]Ra activities were not significantly different than nearshore lagoon waters ($p > 0.05$). [223]Ra and [224]Ra activities in offshore waters at PM were not significantly different than nearshore lagoon waters ($p > 0.05$). At Xcalak [223]Ra and [224]Ra activities offshore were significantly different than nearshore lagoon waters ($p < 0.0003$ and $p < 0.007$, respectively). We were not able to measure the offshore [223]Ra and [224]Ra activities at Sian Ka'an due to logistical constraints that prevented sampling beyond 500 m offshore, thus we use the average offshore activities of the other sites as the offshore end-member for SGD calculations at this site.

End-member activities between the four sampling locations have some similarities but also had some distinct differences (Table 2). The beach groundwater and nearshore surface activities were not significantly different from each other among the four sites, except [223]Ra activities at Cancun ($p < 0.005$) and [224]Ra activities at Xcalak ($p < 0.002$). PM had the highest ojo [223]Ra activity compared to other sites, but the difference among ojos at the different sites was not statistically significant ($p > 0.05$). The [224]Ra to [223]Ra activity ratio ([224]Ra/[223]Ra AR) was different between end-members (Fig. 4). Ojos located at all four sites had significantly lower AR (0.2–5.7) compared to the other end-members, except nearshore AR at Sian Ka'an and beach groundwater AR at Xcalak ($p < 0.05$; Fig. 4). ARs increased in the offshore end-member at all sites in which offshore waters were measured (5.7–105; Fig. 4). Cancun and PM, the two northern sites, had lower [224]Ra activities compared to [223]Ra in ojo waters (AR = 0.9 and 0.7, respectively), and Sian Ka'an and Xcalak had higher [224]Ra activities relative to [223]Ra (AR = 3.1 and 2, respectively), indicative of different aquifer rocks and/or water-rock interaction times (Table 2, Fig. 5). In fact, Xcalak has the highest [224]Ra activities and may represent a distinct groundwater signature (Fig. 5). Average [228]Th activities were significantly greater in ojos (0.5–3.9 dpm 100 L^{-1}) compared to other end-members (0.1–0.3 dpm 100 L^{-1}) at all the sites ($p < 0.05$; Table 2).

3.2. SGD: ojo and beach face

Site-specific ojo discharge was calculated using excess [223]Ra to assess variability in ojo discharge along the coastal region. The ojo SGD fluxes based on excess [223]Ra activities at the different sites ranged between 0.280×10^6 and 11.1×10^6 m^3 d^{-1} per 12 km of shoreline. The two northern sites, Cancun and PM, had lower SGD fluxes, 0.881×10^6 m^3 d^{-1} (73 m^3 d^{-1} m^{-1}) and 0.280×10^6 m^3 d^{-1} (23 m^3 d^{-1} m^{-1}), respectively, compared to Sian Ka'an and Xcalak with fluxes of 11.1×10^6 m^3 d^{-1} (921 m^3 d^{-1} m^{-1}) and 2.58×10^6 m^3 d^{-1} (215 m^3 d^{-1} m^{-1}), respectively (Table 3).

The beach SGD associated with wave set-up and tidal pumping (calculated using analytical solutions) is expected to be similar at

the four sites because they have comparable coastal characteristics. We calculated D_{wave} (Eq. (3)) to be 2.03 m³ d⁻¹ m⁻¹ based on the median values within the possible ranges of K and S, and D_{tide} was estimated to be on the order of 0.66 m³ d⁻¹ m⁻¹ based on Eqs. (4)–(6). The combined first order approximation for saline SGD at each site (SGD_{w+t}) is 2.7 m³ d⁻¹ m⁻¹ (Table 3).

The freshwater discharge calculated using a salinity mass balance (Eq. (7)) at the surf zone (< 20 m) suggests an additional 3.3–8.5 m³ d⁻¹ m⁻¹ of meteoric discharge at the beach face depending on the site (Table 3). Cancun and PM had similar freshwater discharge at the beach face (3.3 and 3.6 m³ d⁻¹ m⁻¹, respectively) and the two southern sites, Sian Ka'an and Xcalak,

had higher freshwater discharge at the beach face (5.9 and 8.5 m³ d⁻¹ m⁻¹, respectively).

3.3. Nutrient concentrations in surface water and groundwater

A summary of average nutrient concentrations ($NO_3^- + NO_2^-$, NH_4^+, PO_4^{3-}, SiO_2) for each site is presented in Table 4. All groundwater samples (ojos and beach groundwater) were elevated in nutrients at all sites compared to surface waters in the coastal area and offshore. NH_4^+ concentrations were high in groundwater sampled from the beach and from ojos compared to surface waters at Cancun, PM, and Xcalak, but similar between ojos and surface waters at Sian Ka'an (both the fresh groundwater and the saline groundwater components in beach groundwater are presented in Table 4). NO_3^- was significantly greater in beach groundwater samples compared to ojos, lagoon and offshore surface water samples at all four sites while NO_2^- was significantly greater in beach sgroundwater only at Cancun and PM ($p < 0.05$). Total dissolved inorganic nitrogen ($DIN = NH_4^+ + NO_3^- + NO_2^-$) concentrations in ojos were similar at PM, Sian Ka'an, and Xcalak (13.6, 10.6, and 10.9 μM respectively) and Cancun had slightly lower average DIN concentrations in ojos (8.8 μM). Average beach groundwater DIN concentrations varied among sites with PM having the highest DIN concentration (336.8 μM) and Cancun and Sian Ka'an with similar low concentrations (~ 49.5 μM). Fresh groundwater at the beach (< 7 salinity) also demonstrated high DIN concentrations at Cancun and Xcalak (264 and 280 μM, respectively). PO_4^{3-} concentrations are relatively low (< 1 μM) in all samples at all the sites. Beach groundwater (especially the fresh groundwater samples) and ojos were significantly enriched with SiO_2 at all sites.

4. Discussion

Considerable discharge of groundwater from ojos occurs along the coast of the eastern Yucatan Peninsula and ranges from 48 m³ d⁻¹ m⁻¹ in the northeast region to 568 m³ d⁻¹ m⁻¹ in the southeast areas. Measured Ra activities in groundwater along with salinity trends indicate that discharge to the coast is taking place from at least two distinct aquifers, an unconfined surficial coastal aquifer (freshwater, low Ra, high NO_3^- and Si) and channelized discharge from aquifers feeding submarine springs (brackish, high Ra, low $^{224/223}$Ra AR, high Si and higher NH_4^+ compared to NO_3^-). Higher Ra activities in groundwater compared to surface water are typical of most coastal sites with saline SGD (e.g. Moore 1996, 1999). The Ra activities in groundwater occurring at the beach face along the Yucatan coast were not significantly higher than nearshore surface waters. The similarity in Ra activities and AR between the beach face groundwater and lagoon waters suggests that Ra in the beach groundwater samples originated from mixing with seawater (i.e. recirculated seawater)
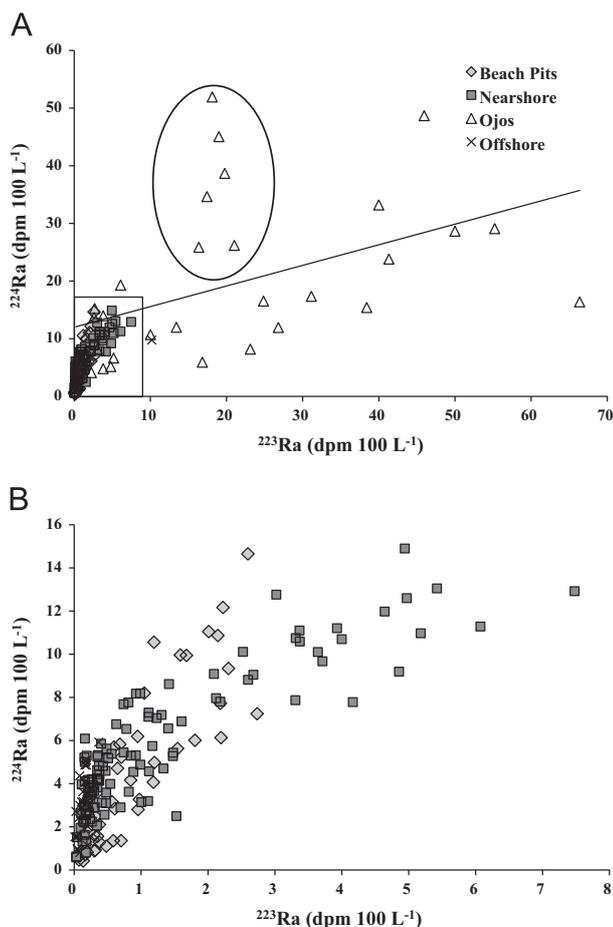
Fig. 5. (a) ^{224}Ra activities vs. ^{223}Ra activities in the different end-members (beach groundwater, nearshore, ojos, and offshore). The circled samples represent the unique signature of ojo activities at Xcalak. (b) ^{224}Ra activities vs. ^{223}Ra activities for the boxed portion of graph (a) representing the lower activities of the beach, surf zone and offshore samples.

Table 3
SGD fluxes from ojos, wave set-up and tidal pumping, and fresh groundwater at each sampling site. The relative contributions in percent of beach and ojo discharge are calculated from the total discharge at each site.

Site	SGD_{ojo}[a]	SGD_{ojo}[b]	SGD_{w+t}[b]	SGD_{fresh}[b]	Total[b]	Relative contribution	
						SGD_{ojo} (%)	SGD_{Beach} (%)
Cancun	0.88	73	2.7	3.3	79.5	**92.4**	**7.6**
PM	0.28	23	2.7	3.6	29.3	**78.5**	**21.5**
SK	11.1	921	2.7	5.9	929.6	**99.1**	**0.9**
Xcalak	2.58	215	2.7	8.5	226.2	**95.0**	**5.0**

[a] Units are m³ d⁻¹ × 10⁶
[b] Units are m³ d⁻¹ m⁻¹ calculated from a shore length of 12000 m at each site.

Table 4
Average and standard deviations (SD) for nutrient concentrations (NO_3^- + NO_2^-, NH_4^+, PO_4^{3-}, SiO_2) and DIN:P ratios of each end-member for each sampling site.

Station/Date		n	N–NH$_4$*		N–NO$_3$*		N–NO$_2$*		P–PO$_4$*		SiO$_2$*		DIN:P
			Ave	SD	Ave	SD	Ave	SD	Ave	SD	Ave	SD	Ave
Cancun/Nov 09	Fresh Beach GW	6	9.0	9.8	233.6	163.2	21.7	15.7	0.7	0.5	112.9	32.1	595
	Beach GW	24	4.3	9.4	43.3	47.3	2.0	2.9	0.8	0.3	36.2	57.5	78.8
	Nearshore	40	0.7	1.4	7.1	6.2	0.9	1.0	0.7	1.0	1.8	3.1	14.4
	Ojos	6	7.0	12.4	1.5	1.3	0.3	0.2	0.8	0.3	30.0	39.0	11.9
	Offshore	13	0.2	0.3	1.9	3.1	0.3	0.4	0.6	0.3	0.6	0.9	3.62
PM/Jan 09	Fresh Beach GW	4	14.2	4.0	14.3	7.4	0.8	0.6	0.8	0.3	94.3	54.1	42.7
	Beach GW	5	3.8	4.9	316.1	181.3	17.6	12.3	0.7	0.1	46.5	20.5	480
	Nearshore	23	2.7	1.5	1.6	6.2	0.2	0.3	0.2	0.0	1.5	0.3	16.7
	Ojos	12	12.5	18.1	1.0	2.3	0.1	0.1	0.5	0.2	15.4	11.8	28.5
	Offshore	9	2.7	6.5	0.8	1.1	0.2	0.4	0.2	0.1	1.8	4.3	4.08
Sian Ka'an/Oct 09	Fresh Beach GW	2	6.3	0.9	26.9	76.9	0.4	0.1	0.7	0.0	101.9	29.3	71.4
	Beach GW	20	17.5	44.5	31.1	23.3	0.9	2.1	0.9	0.2	39.1	43.3	53.5
	Nearshore	36	0.6	0.4	9.3	4.3	0.3	0.0	0.5	0.1	5.1	2.7	22.2
	Ojos	7	0.9	0.8	9.4	13.1	0.3	0.3	0.6	0.1	51.8	28.5	16.5
	Offshore	0	NA	NA	NA	NA	NA	NA	NA	NA	NA	NA	NA
Xcalak/Jan 09	Fresh Beach GW	7	3.7	7.1	275.9	92.1	0.3	0.3	0.4	0.2	81.0	37.8	719
	Beach GW	4	7.0	7.3	116.8	127.1	0.5	0.5	0.3	0.0	21.4	7.3	412
	Nearshore	24	1.8	1.2	0.7	1.0	0.1	0.0	0.2	0.0	5.4	14.1	13.2
	Ojos	6	10.6	4.3	0.2	0.2	0.1	0.0	0.5	0.2	28.6	9.2	23.7
	Offshore	8	1.9	1.1	0.2	0.1	0.1	0.1	0.3	0.1	1.2	0.5	9.14

* Units are in μM

that already had excess Ra activities due to the high discharge from ojos with high Ra activities. ^{223}Ra and ^{224}Ra activities in the nearshore demonstrate mixing of low Ra offshore water and high Ra groundwater from focused discharge at ojos, and minimal contribution from beach discharge (Fig. 5). The low Ra activities of the various potential end-members in this system indicate that discharge from the ojos accounts for the majority of excess Ra activity in coastal waters. Accordingly, using Ra mass balance may be useful for determining fluxes from the ojos but is not sufficient to quantify the lower Ra beach groundwater discharge in this area.

^{223}Ra activities as opposed to ^{224}Ra activities were used for the mass balance model of ojo discharge because ojo water has low ^{224}Ra activities relative to ^{223}Ra activities. In coastal systems, it is expected that the ^{224}Ra/^{223}Ra AR will decrease with distance and time from the source because ^{224}Ra will decay faster than ^{223}Ra. However, along the Yucatan coast, discharge from ojos is characterized by low ^{224}Ra/^{223}Ra AR, even lower than the offshore end-member sampled. This suggests an additional ^{224}Ra source, resulting in a trend towards higher ^{224}Ra/^{223}Ra AR with distance offshore, with minima in the middle of the lagoon near ojo discharge locations. The increase in the offshore AR is not consistent with the box model in which groundwater in the lagoon is the only source of ^{224}Ra to the coastal environment, thereby discounting the use of ^{224}Ra as a tracer of SGD.

^{224}Ra production in offshore waters may be from other channelized discharge high in ^{224}Ra beyond the reef, decay of ^{228}Th from ojos, or decay of ^{228}Ra and ^{228}Th in corals. Other channelized discharge further offshore would be unlikely because if offshore discharge has the same source as ojos it would have a longer pathway and therefore be older with less ^{224}Ra activity. This offshore channelized flow would have to have a different source than the ojos discharging within the reef lagoons. The low AR in the ojo groundwater suggests older groundwater that has undergone some ^{224}Ra decay before discharge and has also possibly interacted with rocks enriched in uranium relative to thorium. U may accumulate in aquifer soils under anoxic conditions resulting in high ^{227}Ac activities supporting high ^{223}Ra activities in groundwater discharging to the coast (Geibert et al., 2008; Moore et al., 2008). The ojo waters also have significantly higher ^{228}Th

compared to other end-members we sampled (Table 2). The high Th activities in the ojo samples may be associated with very small particles that have adsorbed Th. These particles may not have been separated efficiently from the fibers with our coarse filter or washed off efficiently from the fibers with Ra free water before analyses. This fine particle-associated Th may be contributing to the relatively high ARs observed in offshore waters because ^{224}Ra will be generated from ^{228}Th on these particles faster than ^{223}Ra is generated from ^{227}Ac as suggested for other locations (Geibert et al., 2008; Moore et al., 2008). Another likely scenario is the decay of ^{228}Ra and ^{228}Th associated with coral reefs releasing ^{228}Th and ^{224}Ra to offshore waters (Moore et al., 1973).

4.1. SGD: ojos and beach face

Ra activities have been used to calculate SGD occurring in many different nearshore environments (e.g. Moore, 2006 and references therein), and we were able to use Ra activities to calculate ojo discharge to the coastal environment along the Yucatan Peninsula. Using the average ojo ^{223}Ra activities at each site and Eq. (1), we estimate the SGD flux at the four different sites to range between 0.280 to 11.1×10^6 m^3 d^{-1} with the average discharge of 3.7×10^6 m^3 d^{-1} between the beach and the reef crest along 12 km of coastline. The SGD from ojos was greater at the two most southern sites (Sian Ka'an and Xcalak) compared to the northern sites (Cancun and Puerto Morelos). The small amount of Ra contributed from discharge at the beach face was not subtracted in the calculation of ojo discharge. Using the SGD calculated at the beach face and measured Ra activities, it is estimated that the average saline and freshwater flux contributed < 1% to the excess Ra activity in the nearshore environment. The number and size of nearshore ojos remains unknown, however using Ra as a tracer should account for the ojo heterogeneity as these estimates integrate over the spatial scales represented by our coastal "boxes" and temporal scales larger than the water exchange rate in the coastal area.

Other points to consider with these calculations of SGD include diffusion from sediments and the degree of uncertainty in the results stemming from limited data on the residence time of

nearshore waters and variability in measured activities for the end-members. Diffusion from sediments may contribute Ra and nutrients to the nearshore environment. For this study, porewater gradients of Ra were not measured and therefore diffusion from sediments was not calculated. It is possible our estimate of SGD may overestimate the magnitude of advective flux from ojos by not subtracting the diffusive flux of Ra from sediments, but diffusive flux is assumed to be minimal in this high energy, shallow nearshore environment based on studies in other coastal systems. Rama and Moore (1996) calculated that the diffusion of Ra and radon from sediments is negligible in high-energy environments, and Cable and Martin (2008) found the diffusion of radon to account for less than 3% of the total flux from sediments in a nearshore environment. Future studies may consider comparing diffusion and advection processes of nearshore environments along the Yucatan Peninsula to further the understanding of fluxes from the sediments.

The SGD flux estimates also include a degree of error due to the relatively limited available data on water residence times in the nearshore coastal zone for each sampling site and the uncertainty associated with using ^{223}Ra as a tracer. Although multiple studies (Coronado et al., 2007; Kjerfve, 1994; Merino-Ibarra, 1986) suggest lagoon water transport and residence times similar to those used in this study, the water residence may vary between different times of year when calmer periods or storm surges prevail. Coronado et al. (2007) suggests the water residence time of the lagoon at Puerto Morelos may be on the order of two weeks during calm periods and less than one hour during storm surges. If we use the longer water residence time of two weeks, the range of calculated SGD drops to 2.5 to 98×10^3 m^3 d^{-1} for the four sites. The calculated residence time of the Xcalak lagoon is particularly uncertain, and the short residence time determined by scaling the water volume may result in high SGD rates. Improved estimates of lagoon water residence times along the Yucatan coast would greatly improve the accuracy of the SGD calculations for each lagoon. Furthermore, uncertainty in these large-scale SGD estimates is relatively high because of the heterogeneity of Ra activities in this environment. Error was propagated for SGD estimates at each site using summation in quadrature and determined to be 137%, 84%, 142%, and 98% for Cancun, PM, Sian Ka'an, and Xcalak, respectively. This does not include uncertainty associated with the volume or residence time of the nearshore environment because of limited data. The main points of this study (ojo discharge is greater than beach discharge and discharge is greater in the southern sites) are still valid despite the large uncertainty, unless there is a systematic error in the calculation for all the sites.

As previously mentioned SGD$_{w+t}$ is very likely similar among the sites (2.7 m^3 d^{-1} m^{-1}) because the beach face and wave and tide components were the same throughout the sampling region, but the freshwater component of the beach face discharge varies at the different sites (Table 3). Other studies at different locations show greater SGD$_{w+t}$ compared to our findings along the Yucatan Peninsula. In California, de Sieyes et al. (2008) estimated SGD$_{w+t}$ to be on the order of 22.9 m^3 d^{-1} m^{-1} at Stinson Beach, and Boehm et al. (2006) calculated SGD$_{w+t}$ to be 9.5 m^3 d^{-1} m^{-1} at Huntington Beach. The factor that influences the lower SGD$_{w+t}$ in this study is the smaller aquifer thickness of 2 m estimated for the unconfined beach sand compared to ~30 m in the above mentioned studies. Similar to the ojo discharge, the southern sites demonstrated greater freshwater discharge compared to the northern sites, 5.9×10^6 and 8.5×10^6 m^3 d^{-1} m^{-1} in Sian Ka'an and Xcalak compared to 3.3 and 3.6×10^6 m^3 d^{-1} m^{-1}, at Cancun and PM respectively.

When ojo SGD is normalized to the shoreline length (12 km) for each sampling zone, total SGD and the relative contributions of ojo and beach can be calculated per meter of shoreline. Using this calculation the total SGD, including ojos, wave set-up, tidal pumping, and fresh discharge, was greatest at the two southern sites, Sian Ka'an (929.6 m^3 d^{-1} m^{-1}) and Xcalak (226.2 m^3 d^{-1} m^{-1}), and lower at the two northern sites, PM and Cancun (29.3 and 79.5 m^3 d^{-1} m^{-1}, respectively, Table 3). The relative contribution of SGD from ojos was > 90% of the total SGD occurring along the coast except at PM where ojos accounted for ~79% (Table 3).

Factors including the local geology, recharge rates, the degree of fracturing, flow directions and expanse of the coastal estuaries may have influenced the variation in SGD observed among the four sites (Gondwe et al., 2010b; Isphording, 1975). Cancun and PM are located in the Holbox Fracture Zone, and Xcalak is located in the Evaporite Region (Perry et al., 2002). The position of Sian Ka'an in the fracture zones is not clear and may be at a transition between these major hydrogeological terrains (part of the Rio Hondo fracture zone that intersects the Holbox fracture zone near Tulum), or alternatively this area may represent a different groundwater system altogether (Gondwe et al., 2010a).

The general direction of groundwater flow in the Holbox Fracture Zone is predominately to the northeast, and flow in the Evaporite Region is to the southeast and may be better captured at our southern sampling sites (Perry et al., 2002). The presence of groundwater fed swamps, wetlands and some streams in the southern sites is consistent with significant groundwater flow through this region (Gondwe et al., 2010a). Temporal variability in our sampling may also be a factor contributing to the observed differences in SGD since the sites were sampled during different months of the year; however, PM and Xcalak were sampled during the same month (January 2009) and SGD fluxes at PM were an order of magnitude lower than at Xcalak at that time. Thus the seasonal variability appears to have played a minor role in the overall variation of flux. In addition to geological and seasonal effects on SGD, land-use could explain some of the differences observed. There is greater population and potentially greater water usage (i.e. groundwater withdrawal) in the northern part of the peninsula.

Other groundwater studies in the Yucatan Peninsula have reported lower discharge to the coast compared to our estimates (Table 5). Hanshaw and Back (1980) estimated discharge on the order of 8.6×10^6 m^3 km^{-1} yr^{-1} based on a water budget for the entire peninsula, compared to our estimate of 112×10^6 m^3 km^{-1} yr^{-1} (average of ojo SGD at all sites). Other studies using salinity and silica mixing models reported lower groundwater discharge, but these calculations do not consider saline groundwater contribution from ojos (Table 5). Indeed salinity measurements at the ojos are

Table 5
Comparison of groundwater discharge estimates along the Yucatan Peninsula from other studies and this study.

Discharge 10^6 m^3 km^{-1} yr^{-1}	Study	Groundwater Composition	Method
8.6	Hanshaw and Back (1980)	Fresh	Water budget; entire peninsula
0.7–3.9	Smith et al. (1999)	Fresh	Mixing model; salinity and silica
0.5	Hernández-Terrones et al. (2011)	Fresh	Mixing model; salinity and silica
112	This study	Fresh+Saline	^{223}Ra end-member mixing model

consistent with mixing of seawater and meteoric water within the aquifer prior to discharge (Fleury et al., 2007). Flow rates of brackish/saline water in other coastal karst systems have been found to be on the order of $8.6 \times 10^5 \, m^3 \, d^{-1}$ along the coast of Greece (Maurin and Zoelt, 1965) and up to $1.8 \times 10^6 \, m^3 \, d^{-1}$ in the Pupu springs in New Zealand (Williams, 1977). These values are consistent with the extensive intrusion of seawater that can occur in karst aquifers and the large volume of fresh and saline water movement in such systems. The mixed brackish/saline water discharging in many coastal karst systems is chemically different than either the meteoric or surface seawater due to reactions in the subterranean estuary (Slomp and Van Cappellen, 2004; Spiteri et al., 2006) and should be explicitly determined as this water may have significant impact on coastal ecosystems (Moore, 2010). Young et al. (2008) found that the Celestun Lagoon on the northwest corner of the Yucatan Peninsula had different groundwater sources, (1) a low salinity, low radium and high nitrate source, and (2) a brackish source with high radium and less nitrate. The brackish water was described as a mixture of seawater and freshwater with unique chemical characteristics that demonstrate reactions within the aquifer that changes the composition of the water prior to discharge. Both sources of groundwater to the Celestun Lagoon contribute to nutrient loading.

4.2. Nutrient concentrations and fluxes

As with many locations, groundwater along the eastern Yucatan Peninsula is elevated in nutrients compared to surface waters. While all groundwater samples were elevated in nutrients (particularly N and Si) compared to surface water in the lagoon and offshore, differences exist between the beach groundwater and ojos. Specifically, the highest NO_3^- concentrations were found in the unconfined aquifer beach groundwater (particularly the fresh groundwater) at all sites, while NH_4^+ concentrations were similar between ojo and beach groundwater except at Sian Ka'an where beach groundwater had significantly greater NH_4^+ concentrations. Sian Ka'an also had significantly higher ojo and nearshore surface water NO_3^- concentrations compared to the other sites. The difference in nitrogen forms between the beach aquifer and the deeper aquifer (discharging at the offshore ojos) is likely linked to differences in reduction state and related nitrogen transformations in these aquifers: wave and tidal flushing result in an oxygen-rich surficial aquifer, while the deep aquifer likely has lower oxygen levels due to a longer flow path. PO_4^{3-} concentrations were

relatively low in beach groundwater and ojos, likely resulting from the precipitation of P with calcium in carbonate rocks and/or adsorption on Fe–Mn oxide surfaces in the deep and surface aquifers respectively (Fourqurean et al., 1993; Lapointe and Clark, 1992; Zimmerman et al., 1985). SiO_2 is elevated in groundwater samples compared to surface waters and the fresh groundwater at the beach face has significantly higher concentrations compared to ojos and saline beach groundwater (Table 4). Elevated SiO_2 has also been measured in other studies in this region (Hernández-Terrones et al., 2011). It is possible that the high dissolved silica in our samples is related to leaching of silicates from the shallow soil layer or dissolution under reducing conditions in the subterranean estuary (Asano et al., 2003), an observation made in other carbonate dominated karst settings (Fourqurean et al., 1993).

The SGD-associated nutrient fluxes were calculated by subtracting the average surface water nutrient concentrations from the average groundwater nutrient concentrations and multiplying by the calculated SGD fluxes at each site (Fig. 6). Subtracting the surface water nutrient concentration from the groundwater nutrient concentration is a conservative approach and calculates the excess nutrients associated with SGD. The ojos contribute a much greater volume of water compared to the beach discharge, but the beaches often contribute similar nutrient loads due to higher concentrations of nutrients in the unconfined coastal aquifer. Overall, the high volume of ojo discharge dominated SiO_2, PO_4^{3-}, and NH_4^+ fluxes, whereas the $NO_3^- + NO_2^-$ fluxes were mostly contributed by beach groundwater discharge, except at Sian Ka'an. Sian Ka'an had the highest $NO_3^- + NO_2^-$ concentration in ojos and the highest discharge, resulting in the highest $NO_3^- + NO_2^-$ flux and thus higher concentration in coastal water. Fluxes of SiO_2 to coastal waters from SGD associated with the ojos was $> 350 \, mmol \, d^{-1} \, m^{-1}$ of shoreline at all sites (Fig. 6). Sian Ka'an had significantly higher flux of SiO_2 ($> 47 \times 10^3 \, mmol \, d^{-1} \, m^{-1}$) because it had both, a high SGD flux and the highest SiO_2 concentration in ojos compared to other sites. PO_4^{3-} concentrations were similar in ojos at all sites and therefore the fluxes were driven primarily by ojo discharge. Xcalak had the greatest flux of NH_4^+ ($2280 \, mmol \, d^{-1} \, m^{-1}$) from ojo discharge compared to < 950 $mmol \, d^{-1} \, m^{-1}$ at the other sites (Fig. 6). This NH_4^+ flux at Xcalak was driven by high ojo discharge as well as higher ojo NH_4^+ concentrations ($10.6 \, \mu M$). The different nitrogen form contributed from beach groundwater and ojos may influence primary production in the coastal environment as different species have distinct
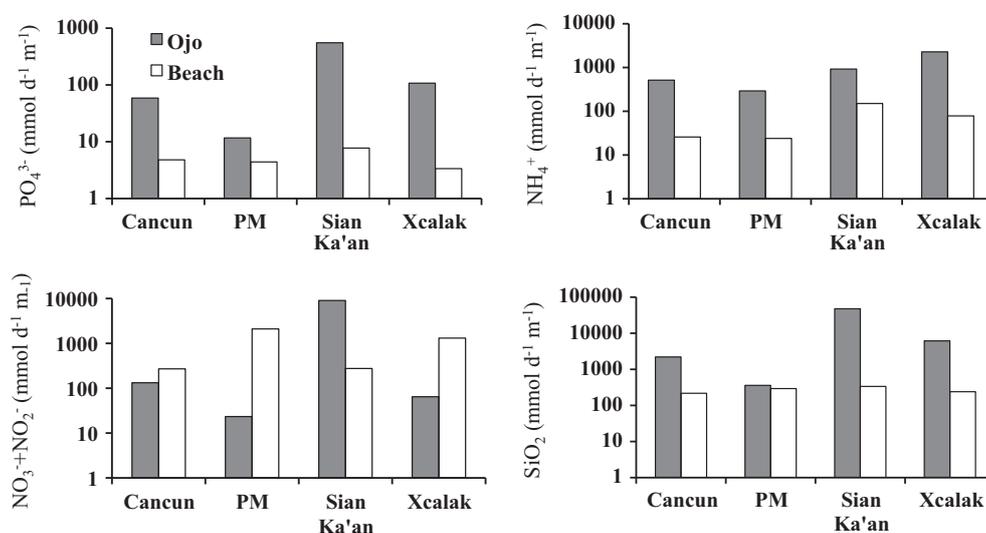

Fig. 6. Nutrient fluxes ($NO_3^- + NO_2^-$, NH_4^+, PO_4^{3-}, SiO_2) from ojos and the beach face at each sampling location. Note units are in $mmol \, d^{-1} \, m^{-1}$ in logarithmic scale to account for the large range of fluxes occurring between ojos and the beach face.

preferences for utilizing the various N forms (Álvarez-Góngora and Herrera-Silveira, 2006; Dugdale et al., 2007).

When considering total dissolved inorganic nitrogen ($NH_4^+ + NO_3^- + NO_2^-$), Sian Ka'an has the highest DIN flux from ojos (7462 mmol d^{-1} m^{-1}) and PM has the highest DIN flux from beach SGD (2122 mmol d^{-1} m^{-1}). Sian Ka'an and Xcalak have the greatest DIN fluxes when considering total SGD flux (ojo and beach), 7888 and 3147 mmol d^{-1} m^{-1}, respectively, to the coast. The high DIN flux from the beach at PM results from the high DIN concentrations (338 μM) in the beach groundwater, whereas the higher volume of discharge from ojos drives greater DIN flux at the southern sites. DIN concentrations in ojos are similar at PM, Sian Ka'an, and Xcalak (13.6, 10.6, and 10.9 μM respectively). Cancun and PM are more populated and it would be expected that these developed sites would have higher DIN fluxes. However, the order of magnitude higher SGD flux in the southern sites resulted in a greater nutrient flux at these sites. This emphasizes the need to identify areas of high discharge and protection of groundwater sources recharging these areas in order to minimize the possibility for eutrophication in the coastal zone. Since this study identified the southern region of the Yucatan Peninsula as having much greater discharge rates compared to the northern sites, we suggest that development and potential contamination in the southern aquifers may have a more negative impact on the marine coast, and any coastal or inland development plans should consider the regional hydrogeology in addition to other factors.

Nutrient loading and the ratio of nutrients delivered to coastal environments can be important to the phytoplankton communities and ecosystem health. Shifts in phytoplankton community structure have been documented in coastal areas impacted by anthropogenic activities that resulted in increased nutrient delivery to coastal waters (Haynes et al., 2007; Chérubin et al., 2008). The ratio of nitrogen to phosphorus (N:P) is also an important factor in phytoplankton composition and productivity in coastal environments. Groundwater often has higher N:P ratio compared to the required N:P ratio by marine phytoplankton around 16:1 ("Redfield ratio", Redfield, 1934). At our sites, the N:P ratio (total DIN to PO_4^{3-} ratio) of beach groundwater was between 53 and 480, considerably above the Redfield ratio, whereas N:P ratios from ojo, nearshore, and offshore waters were not significantly different from each other and fell between 4 and 28, much closer to the Redfield ratio (Table 4). The N:P ratio was greater in fresh groundwater compared to recirculated groundwater at the beach, except at PM where freshwater NO_3^- concentrations were relatively low (Table 4). The nutrient ratios and oxidized forms of nutrients delivered to the surface water along the Yucatan Peninsula coast influence the phytoplankton community structure and result in the dominant presence of diatoms (Troccoli-Ghinaglia et al., 2004, 2010). If the present nutrient contribution to the coastal environment changes, creating a more N-replete system, this may result in a greater abundance of dinoflagellate species as has been observed in other N-replete waters (Gobler and Boneillo, 2003). SGD is an important source of N to the environment and the contribution of SGD (fresh and saline) may influence nutrient ratios in coastal surface waters as well as phytoplankton growth in this region.

4.3. Implications for future development in coastal karstic systems

Research in the Yucatan Peninsula has recognized the need to quantify nutrient pollution and identify nutrient sources to preserve freshwater resources and marine coastal habitats (ArandaCirerol et al., 2011; Gondwe et al., 2011; Herrera-Silveira and Morales-Ojeda, 2009). In the northwest region of the Yucatan Peninsula, a relationship between increased coastal water nutrient concentrations and human activities, including aquaculture, population

density, and tourism has been recognized (ArandaCirerol et al., 2006). More focused studies of nutrient sources in the northwest Yucatan Peninsula showed that livestock was a primary nutrient source (ArandaCirerol et al., 2011). Furthermore, on the west side of the peninsula in Yucatan State, agriculture (N rich fertilizer) was determined to be the main source of elevated NO_3^- in drinking wells (Pacheco et al., 2001).

A main concern throughout the Peninsula, where karst geology results in high recharge and flow rates and few surface water resources exist, is that the freshwater aquifer system that provides drinking water is at risk of pollution. Both, nutrient pollution sources and hydrogeology may vary along the coast, and future studies should consider identifying the sources of nutrient pollution within each aquifer system along the Caribbean coast. Mutchler et al. (2007) found that nutrient concentrations in coastal waters were not different between more developed and less developed areas along the eastern Yucatan coast, similar to our findings. However, more importantly, it has been found that nutrient concentrations and $\delta^{15}N - NO_3^-$ (which suggests anthropogenic sources) were higher in environments with greater freshwater influence rather than amount of development (Mutchler et al., 2007). The southern portion of our study area, Sian Ka'an and Xcalak, have much greater freshwater and total discharge compared to the northern study sites, therefore we suggest contamination of groundwater in the southern sites would have a disproportionally larger negative impact on the coastal environment than the northern sites. Any comparison to impacts (or lack thereof) in the more developed regions to the north would be misleading. Specifically, the southern sites are currently less developed than the northern sites but tourism and development are increasing at dramatic rates. In the northwest region, land use, development, and population density have been identified as the top three nutrient pollution sources to coastal groundwater systems (ArandaCirerol et al., 2011). Although development has not been shown to be directly related to nutrient concentration in marine coastal waters along the eastern Yucatan Peninsula, the high nutrient concentrations in fresh groundwater have been linked to land use and development; thus, population density and tourism along the east coast should not be neglected. Development and tourism have increased four fold along the Rivera Maya from the late 1990s to mid 2000s (Instituto Nacional de Estadistica y Geografia, http://www.inegi.org.mx, Mutchler et al., 2007) and development plans have not taken groundwater fluxes to nearshore ecosystems into account. Based on our data the SGD fluxes rather than nutrient concentrations control the nutrient loads and should not be ignored. In addition, future studies should consider N sources (using natural isotope tracers) and biogeochemical reactions along groundwater flow paths prior to discharge to coastal environments to determine the effect of nutrient pollution in the various aquifers and their potential impacts on the coastal marine environment along the Yucatan Peninsula.

5. Summary

Groundwater discharge from distinct sources (surficial aquifers at the beach face and several deeper aquifers discharging at offshore ojos) was identified along the eastern coast of the Yucatan Peninsula. Discharge from ojos contributes the majority of SGD and a large fraction of nutrient loading; however, SGD at the beach face from the coastal unconfined aquifer delivers more N in the form of NO_3^- to coastal waters at most sites due to higher concentrations in the groundwater. Differences in SGD fluxes between the north and south parts of the eastern peninsula indicate that the geology of the Yucatan Peninsula results in a subsurface water divide near Tulum, with at least two distinct

groundwater sources as well as larger fluxes in the south. The different aquifers are also characterized by distinct Ra activity ratios.

Our data suggest that development in the high discharge areas (southeastern Yucatan Peninsula) may result in higher loading than observed in the north. The SGD fluxes at the Sian Ka'an biosphere reserve are particularly high and it is therefore important to protect and manage this area to ensure good water quality for the coastal environment. This study demonstrates the need to understand the connectivity between inland anthropogenic activities and discharge to the coast through submarine springs and highlights the potential impacts to nearshore coastal environments.

Acknowledgments

References

Álvarez-Góngora, C., Herrera-Silveira, J.A., 2006. Variations of phytoplankton community structure related to water quality trends in a tropical karstic coastal zone. Mar. Pollut. Bull. 52 (1), 48–60.

ArandaCirerol, N., Comín, F., Herrera-Silveira, J., 2011. Nitrogen and phosphorus budgets for the Yucatan littoral: an approach for groundwater management. Environ. Monit. Assess. 172 (1), 493–505.

ArandaCirerol, N., Herrera-Silveira, J., Comín, F., 2006. Nutrient water quality in a tropical coastal zone with groundwater discharge, northwest Yucatan, Mexico. Estuar. Coast. Shelf Sci. 68, 445–454, http://dx.doi.org/10.1016/j.ecss.2006.02.015.

Asano, Y., Uchida, T., Ohte, N., 2003. Hydrologic and geochemical influences on the dissolved silica concentration in natural water in a steep headwater catchment. Geochim. Cosmochim. Acta 67, 1973–1989, http://dx.doi.org/10.1016/S0016-7037(02)01342-X.

Back, W., Hanshaw, B.B., 1970. Comparison of chemical hydrogeology of the carbonate peninsulas of Florida and Yucatan. J. Hydrol. 10 (4), 330–368.

Beddows, P.A., Smart, P.L., Whitaker, F.F., Smith, S.L., 2002. Density stratified groundwater circulation on the Caribbean coast of the Yucatan Peninsula, Mexico. In: Martin, J.B., Wicks, C.M., Sasowsky, I.D. (Eds.), Hydrogeology and Biology of Post-Paleozoic Carbonate Aquifers. Karst Waters Institute Special Publication, Charles Town, West Virginia, vol. 7, pp. 129–134.

Beddows, P.A., Smart, P.L., Whitaker, F.F., Smith, S.L., 2007. Decoupled fresh–saline groundwater circulation of a coastal carbonate aquifer: spatial patterns of temperature and specific electrical conductivity. J. Hydrol. 346 (1), 18–32.

Boehm, A.B., Paytan, A., Shellenbarger, G.G., Davis, K.A., 2006. Composition and flux of groundwater from a California beach aquifer: implications for nutrient supply to the surf zone. Cont. Shelf Res. 26 (2), 269–282.

Boehm, A., Shellenbarger, G., Paytan, A., 2004. Groundwater discharge: a potential association with fecal indicator bacteria in the surf zone. Environ. Sci. Technol. 38, 3558–3566.

Bonacci, O., Roje-Bonacci, T., 1997. Seawater intrusion in coastal karst springs: example of the Blaž Spring (Croatia). Hydrol. Sci. J. 42 (1), 89–100.

Burnett, W.C., Bokuniewicz, H., Huettel, M., Moore, W.S., Taniguchi, M., 2003. Groundwater and pore water inputs to the coastal zone. Biogeochemistry 66, 3–33.

Cable, J.E., Martin, J.B., 2008. In situ evaluation of nearshore marine and fresh porewater transport into Flamengo Bay, Brazil. Estuar. Coast. Shelf Sci. 76, 473–483.

Chavez-Guillen, R., 1986. Sinopsis geohidrologica del estado de Quintana Roo: Mexico City, SARH, 46p. and 7 plates.

Chérubin, L.M., Kuchinke, C.P., Paris, C.B., 2008. Ocean circulation and terrestrial runoff dynamics in the Mesoamerican region from spectral optimization of SeaWiFS data and a high resolution simulation. Coral Reefs 27 (3), 503–519.

Corbett, D.R., Chanton, J., Burnett, W., Dillon, K., Rutkowski, C., Fourqurean, J.W., 1999. Patterns of groundwater discharge into Florida Bay. Limnolo. Oceanogr. 44, 1045–1055.

Coronado, C., Candela, J., Iglesias-Prieto, R., Sheinbaum, J., López, M., Ocampo-Torres, F.J., 2007. On the circulation in the Puerto Morelos fringing reef lagoon. Coral Reefs 26 (1), 149–163.

de Sieyes, N.R, Yamahara, K.M., Layton, B.A., Joyce, E.H., Boehm, A.B., 2008. Submarine discharge of nutrient-enriched fresh groundwater at Stinson Beach, California is enhanced during neap tides. Limnol. Oceanogr. 53, 1434–1445.

Domenico, P.A., Schwartz, F.W., 1990. Physical and Chemical Hydrogeology. Wiley, New York p. 824

Dugdale, R.C., Wilkerson, F.P., Hogue, V.E., Marchi, A., 2007. The role of ammonium and nitrate in spring bloom development in San Francisco Bay. Estuar. Coast. Shelf Sci. 73, 17–29.

Fleury, P.,M., Bakalowicz, G., de Marsily, 2007. Submarine spring and coastal karst aquifers: a review. J. Hydrol. 339, 79–92.

Fourqurean, J.W., Jones, R.D., Zieman, J.C., 1993. Process influencing water column nutrient characteristics and phosphorus limitation of phytoplankton biomass in Florida Bay, FL, USA: inferences from spatial distributions. Estuar. Coast. Shelf Sci. 36 (3), 295–314.

Garcia-Solsona, E., Garcia-Orellana, J., Masque, P., Dulaiova, H., 2008. Uncertainties associated with ^{223}Ra and ^{224}Ra measurements in water via a Delayed Coincidence Counter (RaDeCC). Mar. Chem. 109 (3), 198–219, http://dx.doi.org/10.1016/j.marchem.2007.11.006.

Geibert, W., Charette, M., Kim, G., Moore, W.S., Street, J., Young, M., Paytan, A., 2008. The release of dissolved actinium to the ocean: a global comparison of different end-members. Mar. Chem. 109 (3), 409–420, http://dx.doi.org/10.1016/j.marchem.2007.07.005.

Gobler, C.J., Boneillo, G.E., 2003. Impacts of anthropogenically influenced groundwater seepage on water chemistry and phytoplankton dynamics within a coastal marine system. Mar. Ecol. Prog. Ser. 255, 101–114.

Gondwe, B.R., Hong, S.H., Wdowinski, S., Bauer-Gottwein, P., 2010b. Hydrologic dynamics of the ground-water-dependent Sian Ka'an Wetlands, Mexico, derived from InSAR and SAR data. Wetlands 30 (1), 1–13.

Gondwe, B., Lerer, S., Stisen, S., Marín, J., Rebolledo-Vieyra, M., Merediz-Alonso, G., Bauer-Gottwein, P., 2010a. Hydrogeology of the southeastern Yucatan Peninsula: new insights from water level measurements, geochemistry, geophysics and remote sensing. J. Hydrol. 389 (1), 1–17, http://dx.doi.org/10.1016/j.jhydrol.2010.04.044.

Gondwe, B., Merediz-Alonso, G., Bauer-Gottwein, P., 2011. The influence of conceptual model uncertainty on management decisions for a groundwater-dependent ecosystem in karst. J. Hydrol. 400, 24–40, http://dx.doi.org/10.1016/j.jhydrol.2011.01.023.

Haynes, D., Brodie, J., Waterhouse, J., Bainbridge, Z., Bass, D., Hart, B., 2007. Assessment of the water quality and ecosystem health of the Great Barrier Reef (Australia): conceptual models. Environ. Manag. 40 (6), 993–1003.

Hanshaw, B.B., Back, W., 1980. Chemical mass-wasting of the northern Yucatan Peninsula by groundwater dissolution. Geology 8, 222–224.

Hernández-Terrones, L, Rebolledo-Vieyra, M., Merino-Ibarra, M., Soto, M., Le-Cossec, A., Monroy-Rios , E., 2011. Groundwater pollution in a karstic region (NE Yucatan): baseline nutrient content and flux to coastal ecosystems. Water Air Soil Pollut. 218 (1–4), 517–528, http://dx.doi.org/ 10.1007/s11270-010-0664-x.

Herrera-Silveira, J., 1998. Nutrient-phytoplankton production Relationship in a groundwater influenced tropical coastal lagoon. Aquat. Ecosyst. Health Manag. 1 (3–4), 353–372.

Herrera-Silveira, J.A., Morales-Ojeda, S.M., 2009. Evaluation of the health status of a coastal ecosystem in southeast Mexico: assessment of water quality, phytoplankton and submerged aquatic vegetation. Mar. Pollut. Bull. 59, 72–86, http://dx.doi.org/10.1016/j.marpolbul.2008.11.017.

Instituto Nacional de Estadistica y Geografia, www.inegi.org.mx.

Isphording, W.C., 1975. The physical geology of the Yucatan. Trans. Gulf Coast Assoc. Geol. Soc. 25, 231–262.

Kjerfve, B., 1994. Coastal Oceanographic Characteristics: Cancun-Tulum Corridor, Quintana Roo. Final Report, Programa de Ecologia, Pesquerias y Oceanografia del Golfo de Mexico, Universidad Autonoma de Campeche, pp. 1–35.

Knee, K.L., Street, J.H., Grossman, E.E., Boehm, A.B., Paytan, A., 2010. Nutrient inputs to the coastal ocean from submarine groundwater discharge in a groundwater-dominated system: relation to land use (Kona coast, Hawaii, U.S.A.). Limnol. Oceanogr. 55 (3), 1105–1122.

Krekeler, M.P.S., Argyilan, E.P., Lepp, J., Kearns, L.E., 2009. Investigation of calcareous beach sands in the Akumal and Tulum areas for use in constructed wetlands, Eastern Yucatan Peninsula. Environ. Earth Sci. 59 (2), 411–420, http://dx.doi.org/10.1007/s12665-009-0039-z.

Lapointe, B., Clark, M., 1992. Nutrient inputs from the watershed and coastal eutrophication in the Florida keys. Estuar. Coasts 15, 465–476.

Li, L, Barry, D.A., Stagnitti, F., Parlange, J., 1999. Submarine groundwater discharge and associated chemical input to a coastal sea. Water Resour. Res. 35, 3253–3259.

Longuet-Higgins, M.S., 1983. Wave set-up, percolation and undertow in the surf zone. Proc. R. Soc. London: Ser. A Math. Phys. Sci. 390, 283–291.

Maurin, V., Zoelt, J., 1965. Salt Water Encroachment in the Low Altitude Karst Water Horizons of the Island of Kephallinia (Ionian Islands), Hydrologie des roches fissure´es, vol. 2, pp. 423–438.

McWhorter, D., Sunada, D.K., 1977. Ground-Water Hydrology and Hydraulics. Water Resources PublicationsFort Collins, CO, pp. 1–290

Meacham, S., 2007. Freshwater resources in the Yucatan Peninsula. In: Holliday, L., Marin, L., Vaux (Eds.), Sustainable Management of Groundwater in Mexico: Proceedings of a Workshop. National Academies Press, Washington, D.C. pp. 6–12.

Merino-Ibarra, M., 1986. Aspectos de la circulación costera superficial del Caribe Mexicano con base en observaciones utilizando tarjetas de deriva. In: Anales del Instituto de Ciencias del Mar y Limnología, Universidad Nacional Autónoma de México, vol. 13, pp. 31–46.

Metcalfe, C.D., Beddows, P.A., Bouchot, G.G., Metcalfe, T.L., Li, H., Van Lavieren, H., 2011. Contaminants in the coastal karst aquifer system along the Caribbean coast of the Yucatan Peninsula, Mexico. Environ. Pollut. 159 (4), 991–997, http://dx.doi.org/10.1016/j.envpol.2010.11.031.

Michael, H.A., Mulligan, A.E., Harvey, C.F., 2005. Seasonal oscillations in water exchange between aquifers and the coastal ocean. Nature 436, 1145–1148, http://dx.doi.org/10.1038/nature03935.

Moore, W.S., 1976. Sampling ^{228}Ra in the deep ocean. Deep Sea Res. Oceanogr. Abstr. 23, 647–651.

Moore, W.S., 1996. Large groundwater inputs to coastal waters revealed by ^{226}Ra enrichments. Nature 380, 612–614.

Moore, W.S., 1999. The subterranean estuary: a reaction zone of ground water and seawater. Mar. Chem. 65, 111–125.

Moore, W.S., 2000. Ages of continental shelf water determined from ^{223}Ra and ^{224}Ra. J. Geophys. Res. 105, 22,117–22,122.

Moore, W.S., 2006. Radium isotopes as tracers of submarine groundwater discharge in Sicily. Cont. Shelf Res. 26, 852–861, http://dx.doi.org/10.1016/j.csr.2005.12.004.

Moore, W.S., Ussler, W., Paull, C.K., 2008. Short-lived radium isotopes in the Hawaiian margin: evidence for large fluid fluxes through the Puna Ridge. Mar. Chem. 109, 421–430, http://dx.doi.org/10.1016/j.marchem.2007.09.010.

Moore, W.S., 2010. The effect of submarine groundwater discharge on the ocean. Annu. Rev. Mar. Sci. 2, 59–88, http://dx.doi.org/10.1146/annurev-marine-120308-081019.

Moore, W.S., Arnold, R., 1996. Measurement of ^{223}Ra and ^{224}Ra in coastal waters using a delayed coincidence counter. J. Geophys. Res. 101, 1321–1329.

Moore, W.S., Krishnaswami, S., and Bhat, S.G., 1973. Radiometric determinations of coral growth rates. Bulletin of Marine Science, 23 (2), 157-176.

Moore, Y.H., Stoessell, R.K., Easley, D.H., 1993. Freshwater-seawater relationship within a groundwater flow system, Northeastern coast of the Yucatan Peninsula – reply. Ground Water 31, 321–322.

Mutchler, T., Dunton, K.H., Townsend-Small, A., Fredriksen, S., Rasser, M.K., 2007. Isotopic and elemental indicators of nutrient sources and status of coastal habitats in the Caribbean Sea, Yucatan Peninsula, Mexico. Estuar. Coast. Shelf Sci. 74, 449–457.

Núnez-Lara, E., Ernesto Arias-González, J., Legendre, P., 2005. Spatial patterns of Yucatan reef fish communities: testing models using a multi-scale survey design. J. Exp. Mar. Biol. Ecol. 324 (2), 157–169.

Pacheco, A.J., Cabrera, S.A., 1997. Groundwater contamination by nitrates in the Yucatan Peninsula, Mexico. Hydrogeol. J. 5, 47–53.

Pacheco, J., Marín, L., Cabrera, A., Steinich, B., Escolero, O., 2001. Nitrate temporal and spatial patterns in 12 water-supply wells, Yucatan, Mexico. Environ. Geol. 40, 708–715.

Paytan, A., Shellenbarger, G.G., Street, J.H., Gonneea, M.E., Davis, K., Young, M.B., Moore, W.S., 2006. Submarine groundwater discharge: an important source of new inorganic nitrogen to coral reef ecosystems. Limnol. Oceanogr. 51, 343–348.

Perry, E., Marin, L., McClain, J., Velazquez, G., 1995. Ring of cenotes (sinkholes), northwest Yucatan, Mexico: its hydrogeologic characteristics and possible association with the Chicxulub impact crater. Geology 23 (1), 17–20.

Perry, E.C., Swift, J., Gamboa, J., Reeve, A., Sanborn, R., Marin, L., Villasuso, M., 1989. Geologic and environmental aspects of surface cementation, north coast, Yucatan, Mexico. Geology 17 (9), 818–821.

Perry, E., Velazquez-Oliman, G., Marin, L., 2002. The hydrogeochemistry of the karst aquifer system of the northern Yucatan Peninsula, Mexico. Int. Geol. Rev. 44, 191–221.

Rama, Moore, W.S., 1996. Using the radium quartet for evaluating groundwater input and water exchange in salt marshes. Geochim. Cosmochim. Acta 60, 4645–4652.

Redfield, A.C., 1934. On the proportions of organic derivatives in seawater and their relation to the composition of plankton. In: Daniel, R.J., (Ed.), James Johnson Memorial Volume, Liverpool Univ. Press, Liverpool, pp. 177–192.

Ruiz-Renteria F, van Tussenbroek B.I., Jordan-Dahlgren E., 1998. Puerto Morelos, Quintana Roo, Mexico. In CARICOMP: Caribbean Coral Reef, Seagrass, and Mangrove Sites. Special Report UNESCO, Paris, pp. 57–66.

Robinson, C., Li, L, Barry, D.A., 2007. Effect of tidal forcing on a subterranean estuary. Adv. Water Resour. 30, 851–865, http://dx.doi.org/10.1016/j.advwatres.2006.07.006.

Slomp, C.P., Van Cappellen, P., 2004. Nutrient inputs to the coastal ocean through submarine groundwater discharge: controls and potential impact. J. Hydrol. 295, 64–86.

Smith, S.V., Camacho-Ibar, V., Herrera-Silveira, J.A., Valdes, D., Merino, D.M., Buddemeier, R.W., 1999. Quantifying groundwater flow using water budgets and multiple conservative tracers, 96–105. In: Smith, S.V., Marshall Crossland, J.I., Crossland, C.J.(Ed.), Mexican and Central American Coastal Lagoon Systems: Carbon, Nitrogen, and Phosphorus Fluxes (Regional Workshop II), LOICZ Reports & Studies No. 13, Texel, The Netherlands.

Spiteri, C., Regnier, P., Slomp, C.P., Charette, M.A., 2006. pH-Dependent iron oxide precipitation in a subterranean estuary. J. Geochem. Explor. 88 (1), 399–403.

Steinich, B., Marín, L.E., 1996. Hydrogeological Investigations in Northwestern Yucatan, Mexico, using Resistivity Surveys. Ground Water 34 (4), 640–646.

Stoessell, R.K., Ward, W.C., Ford, B.H., Schuffert, J.D., 1989. Water chemistry and $CaCO_3$ dissolution in the saline part of the open-flow mixing zone, coastal Yucatan Peninsula, Mexico. Geol. Soc. Am. Bull. 101, 159–169.

Taniguchi, M., Ishitobi, T., Shimada, J., 2006. Dynamics of submarine groundwater discharge and freshwater–seawater interface. J. Geophys. Res. 111, 1978–2012, http://dx.doi.org/10.1029/2005JC002924.

Troccoli-Ghinaglia, L., Herrera-Silveira, J.A., Comín, F.A., 2004. Structural variations of phytoplankton in the coastal seas of Yucatan, Mexico. Hydrobiologia 519 (1), 85–102.

Troccoli-Ghinaglia, L., Herrera-Silveira, J.A., Comín, F.A., Díaz-Ramos, J.R., 2010. Phytoplankton community variations in tropical coastal area affected where submarine groundwater occurs. Cont. Shelf Res. 30 (20), 2082–2091.

Villasuso, M.J., Ramos, R.M., 2000. A conceptual model of the aquifer of the Yucatan Peninsula. Lutz, W., Prieto L, Sanderson, W.C. (Eds.), Population, Development, and Environment on the Yucatan Peninsula: From Ancient Maya to 2030. International Institute for Applied Systems Analysis.

Webster, I.T., Hancock, G.J., Murray, A.S., 1995. Modelling the effect of salinity on radium desorption from sediments. Geochim. Cosmochim. Acta 59 (12), 2469–2476.

Williams, P.W., 1977. Hydrology of the Walkoropupu Springs: a major tidal karst resurgence in northwest Nelson (New Zealand). J. Hydrol. 35 (1), 73–92.

Young, M.B., Gonneea, M.E., Fong, D.A., Moore, W.S., Herrera-Silveira, J., Paytan, A., 2008. Characterizing sources of groundwater to a tropical coastal lagoon in a karstic area using radium isotopes and water chemistry. Mar. Chem. 109, 377–394.

Zimmerman, C.F., Montgomery, J.R., Carlson, P.R., 1985. Variability of dissolved reactive phosphate flux rates in nearshore estuarine sediments: effects of groundwater flow. Estuaries 8, 228–236.